Computer Physics Communications 138 (2001) 53–68

Computer Physics Communications

www.elsevier.com/locate/cpc

Application of the Characteristic Bisection Method for locating and computing periodic orbits in molecular systems

M.N. Vrahatis [a,*], A.E. Perdiou [a], V.S. Kalantonis [a], E.A. Perdios [b], K. Papadakis [b], R. Prosmiti [c,1], S.C. Farantos [c,2]

[a] *Department of Mathematics and University of Patras Artificial Intelligence Research Center (UPAIRC), GR-261 10 Patras, Greece*
[b] *Department of Engineering Sciences, University of Patras, GR-26110 Patras, Greece*
[c] *Department of Chemistry, University of Crete, Iraklion, Crete 71110, Greece*

Received 24 November 2000; accepted 10 March 2001

Dedicated to the memory of Chronis Polymilis (1946–2000)

Abstract

The Characteristic Bisection Method for finding the roots of non-linear algebraic and/or transcendental equations is applied to LiNC/LiCN molecular system to locate periodic orbits and to construct the continuation/bifurcation diagram of the bend mode family. The algorithm is based on the Characteristic Polyhedra which define a domain in phase space where the topological degree is not zero. The results are compared with previous calculations obtained by the Newton Multiple Shooting algorithm. The Characteristic Bisection Method not only reproduces the old results, but also, locates new symmetric and asymmetric families of periodic orbits of high multiplicity.

PACS: 39.30; 31.15.-p; 02.70.-c; 05.45.+b

Keywords: Characteristic Bisection Method; Molecular systems; Dynamical systems; Periodic orbits; Poincaré map; Topological degree theory

1. Introduction

Periodic orbits play a major role in assigning the vibrational levels of highly excited polyatomic molecules [1–3]. One of the research contributions of our late colleague *Chronis Polymilis* to whom this article is dedicated, was on this subject [4,5]. HCP [6] and acetylene [7,8] are two well studied molecules for which the assignment of their complicated highly resolved vibrational spectra were elucidated by locating the proper families of periodic orbits.

* Corresponding author.
E-mail addresses: vrahatis@math.upatras.gr (M.N. Vrahatis), aperdiou@math.upatras.gr (A.E. Perdiou), vkalan@math.upatras.gr (V.S. Kalantonis), e.perdios@des.upatras.gr (E.A. Perdios), k.papadakis@des.upatras.gr (K. Papadakis), rita@iesl.forth.gr (R. Prosmiti), farantos@iesl.forth.gr (S.C. Farantos).
[1] Current address: Instituto de Matematicas y Fisica Fundamental, Consejo Superior de Investigaciones Cientificas, Serrano 123, 28006 Madrid, Spain.
[2] Also at Institute of Electronic Structure and Laser, Foundation for Research and Technology, Hellas, Iraklion 711 10, Crete, Greece.

0010-4655/01/$ – see front matter
PII: S0010-4655(01)00190-4

Based on the assumption which is supported by semiclassical theories [9,10], for the localization of quantum eigenfunctions or superpositions of them along stable or the least unstable periodic orbits, families of periodic orbits and their associated continuation/bifurcation diagrams constructed by varying a parameter of the system can be used to unravel the complicate dynamics of the molecule [1]. HCP is a good example for predicting motions entangled with the isomerization of the molecule by using saddle node bifurcations of periodic orbits [11,12].

In general, analytic expressions for evaluating periodic orbits are not available. Also, as it is well known, the numerical techniques for computing families of periodic orbits (symmetric or asymmetric) is a time consuming procedure. The main difficulty for the computation of a family of periodic orbits of a given period is the determination of an individual member of this family. We have successfully applied Newton algorithms in conjunction to Multiple Shooting techniques [13,14]. The latter allows a better sampling of phase space which guarantees convergence to a nearby periodic orbit even for those of relatively long period. In general, an individual member can be determined by starting from an equilibrium point of the system under consideration. In the case of symmetric orbits another approach is to create a grid in the (E, R) plane where E is the energy [15] and R determines distances (independent coordinates). In this case an individual member can be determined using a constant value of E.

In this paper, we investigate a new technique to compute an individual member of any family in molecular systems, even in cases where the orbit (whether stable or unstable) is asymmetric and/or of high multiplicity. The approach is based on the Poincaré map Φ on a surface of section. We say that $\mathbf{X} = (x_1, x_2, \ldots, x_n)^\top$ is a *fixed point* or a *periodic orbit* of Φ if $\Phi(\mathbf{X}) = \mathbf{X}$ and a *periodic orbit of period* p if:

$$\mathbf{X} = \Phi^p(\mathbf{X}) \equiv \underbrace{\Phi\big(\Phi(\cdots(\Phi(\mathbf{X}))\cdots)\big)}_{p \text{ times}}. \tag{1}$$

It is evident that the problem of computing an individual member of a specific family of periodic orbits is equivalent to the problem of evaluating the corresponding fixed point of the Poincaré map. Traditional iterative schemes such as Newton's method and related classes of algorithms [16,17] often fail to converge to a specific periodic orbit since their convergence is almost independent of the initial guess. Thus, while there exist several periodic orbits close to each other, which may all be desirable for applications, it is difficult for these methods to converge to the specific periodic orbit. Moreover, these methods are affected by the imprecision of the mapping evaluations. It may also happen that these methods fail due to the nonexistence of derivatives or poorly behaved partial derivatives [16,17]. This can be easily verified by studying the basins of convergence of these methods which exhibit a fractal-like structure [18].

It is obvious that there is a need in investigating new methods for locating periodic solutions of the molecular equations of motion. To this end, we explore a new numerical method for computing periodic orbits (stable or unstable) of any period and to any desired accuracy. This method exploits topological degree theory to provide a criterion for the existence of a periodic orbit of an iterate of the mapping within a given region. In particular, the method constructs a polyhedron using the pth iterate in such a way that the value of the topological degree of the mapping relative to this polyhedron is ± 1, which means that there exists a periodic orbit within this polyhedron. Then, it repeatedly subdivides its edges (and/or its diagonals) so that the new polyhedron also retains this property (of the existence of a periodic orbit within it) without making any computation of the topological degree. These subdivisions take place iteratively until a periodic point is computed to a predetermined accuracy. More details of this method can be found in [19].

This method becomes especially promising for the computation of high period orbits (stable or unstable) where other more traditional approaches (like Newton's method, etc.) cannot easily distinguish among the closely neighboring periodic orbits. Moreover, this method is particularly useful, since the only computable information it requires is the algebraic signs of the components of the mapping. Thus, it is not affected by the imprecisions of the mapping evaluations. Recently, this method has been applied successfully to various difficult problems; see, for example, [20–26].

In the present paper, we employ this method to compute individual members of families of periodic orbits of the LiNC/LiCN molecule. An extensive study of this system was carried out in the past [27]. By constructing continuation/bifurcation diagrams of families of periodic orbits the spectroscopy and dynamics for this species were deduced and compared with accurate quantum mechanical calculations up to 13 000 cm^{-1} and using a 2D potential function. The purpose of the present article is to apply and test the Characteristic Bisection Method (CBM) in locating and computing periodic orbits for the LiNC molecule.

The paper is organized as follows. In the next section we briefly present the features of the LiNC/LiCN model. In Section 3 we present a classical approach to create families of periodic orbits when an individual member of this family is given. In Section 4, we present the proposed method for computing within a given box individual members of families of periodic orbits of a given period. In Section 5, we apply the proposed method to the computation of individual members of families of periodic orbits of LiNC model. The paper ends with some concluding remarks.

2. LiNC/LiCN model

We employ the same potential energy surface used in the study by Prosmiti et al. [27]. This is a Hartree–Fock electronic potential computed by Essers et al. [28]. The same potential was used in all quantum mechanical calculations for the two-dimensional vibrational problem with fixed the CN^- bond. The Hamiltonian is expressed in Jacobi coordinates, (R, θ), where R is the distance of Li^+ from the center of mass of CN^-, and θ is the angle between R and the bond length of CN^-, r, which is fixed at $2.186a_0$.

The Hamiltonian has the form:

$$H = \frac{P_R^2}{2\mu_1} + \left(\frac{1}{\mu_1 R^2} + \frac{1}{\mu_2 r^2}\right)\frac{P_\theta^2}{2} + V(R,\theta), \tag{2}$$

where $\mu_1^{-1} = m_{\mathrm{Li}}^{-1} + (m_{\mathrm{C}} + m_{\mathrm{N}})^{-1}$, $\mu_2^{-1} = m_{\mathrm{C}}^{-1} + m_{\mathrm{N}}^{-1}$ are the reduced masses, and m_{C}, m_{N}, and m_{Li} are the atomic masses.

The potential surface, $V(R,\theta)$, has two minima with linear geometries: the absolute minimum is for LiNC at ($R = 4.3487a_0$, $\theta = \pi$), and the relative minimum is for LiCN at ($R = 4.7947a_0$, $\theta = 0$) with energy 2281 cm^{-1} above the LiNC minimum. The barrier of isomerization between these two minima is at 3455.5 cm^{-1} and with the geometry ($R = 4.2197a_0$, $\theta = 0.91799$). Also, there is a plateau in the LiNC well at 1207 cm^{-1} above the absolute minimum, and with geometry ($R = 3.65a_0$, $\theta = 1.92$).

The Multiple Shooting Method for calculating periodic orbits was described in [1,14]. This is a general procedure for locating symmetric or asymmetric periodic orbits.

3. Creating families of periodic orbits

Next we give an efficient method for finding periodic orbits using the classical approach of Newton technique as well as for carrying out the continuation of the family with respect to the period and the stability analysis of periodic orbits. This method is applicable when an individual member of the family is given.

If $(R_0, \theta_0, P_{R_0}, P_{\theta_0})$ are the initial conditions of an orbit at $t_0 = 0$, then, the periodicity conditions that must be satisfied are:

$$\begin{aligned}
&R(R_0, \theta_0, P_{R_0}, P_{\theta_0}, T) = R_0,\\
&\theta(R_0, \theta_0, P_{R_0}, P_{\theta_0}, T) = \theta_0,\\
&P_R(R_0, \theta_0, P_{R_0}, P_{\theta_0}, T) = P_{R_0},\\
&P_\theta(R_0, \theta_0, P_{R_0}, P_{\theta_0}, T) = P_{\theta_0}.
\end{aligned} \tag{3}$$

Now since in this paper the symmetric periodic orbits which we have computed are with respect to the R-axis then Eqs. (3) for the half period become:

$$\begin{aligned} &\theta(R_0, P_{\theta_0}, T_1) = \pi, \\ &P_R(R_0, P_{\theta_0}, T_1) = 0, \end{aligned} \tag{4}$$

where $T_1 = T/2$. Consider the corrections ΔR_0, ΔP_{θ_0} and ΔT_1 of R_0, P_{θ_0} and T_1, respectively, which satisfy relations (4). Thus:

$$\begin{aligned} &\theta(R_0 + \Delta R_0, P_{\theta_0} + \Delta P_{\theta_0}, T_1 + \Delta T_1) = \pi, \\ &P_R(R_0 + \Delta R_0, P_{\theta_0} + \Delta P_{\theta_0}, T_1 + \Delta T_1) = 0. \end{aligned} \tag{5}$$

Next, using Taylor series we expand Eqs. (5) around R_0, P_{θ_0}, T_1 and by neglecting all the nonlinear terms, we finally obtain that:

$$\begin{aligned} &\frac{\partial\theta}{\partial R_0}\Delta R_0 + \frac{\partial\theta}{\partial P_{\theta_0}}\Delta P_{\theta_0} + \frac{\partial\theta}{\partial t}\Delta T_1 = \pi - \theta(T_1), \\ &\frac{\partial P_R}{\partial R_0}\Delta R_0 + \frac{\partial P_R}{\partial P_{\theta_0}}\Delta P_{\theta_0} + \frac{\partial P_R}{\partial t}\Delta T_1 = -P_R(T_1). \end{aligned} \tag{6}$$

By integrating relations (6) and by keeping t constant, that is $\Delta T_1 = 0$, we have:

$$\begin{bmatrix} \dfrac{\partial\theta}{\partial R_0} & \dfrac{\partial\theta}{\partial P_{\theta_0}} \\ \dfrac{\partial P_R}{\partial R_0} & \dfrac{\partial P_R}{\partial P_{\theta_0}} \end{bmatrix} \begin{bmatrix} \Delta R_0 \\ \Delta P_{\theta_0} \end{bmatrix} = \begin{bmatrix} \pi - \theta(T_1) \\ -P_R(T_1) \end{bmatrix}. \tag{7}$$

It is evident that using the corrections ΔR_0 and ΔP_{θ_0} we are able to obtain the new vector of initial conditions $(R_0 + \Delta R_0, P_{\theta_0} + \Delta P_{\theta_0})^\top$. Next, we integrate the equations of motion with the new initial conditions and we repeat this procedure until the periodicity conditions (4) are satisfied with the desired accuracy.

When a periodic orbit ($\theta = \pi$, $P_R = 0$) has been computed, by changing ΔT_1 with an arbitrary small constant ε we are able to obtain from Eqs. (6) that:

$$\begin{bmatrix} \dfrac{\partial\theta}{\partial R_0} & \dfrac{\partial\theta}{\partial P_{\theta_0}} \\ \dfrac{\partial P_R}{\partial R_0} & \dfrac{\partial P_R}{\partial P_{\theta_0}} \end{bmatrix} \begin{bmatrix} \delta R_0 \\ \delta P_{\theta_0} \end{bmatrix} = \begin{bmatrix} \pi - \varepsilon\dfrac{\partial\theta}{\partial t} \\ -\varepsilon\dfrac{\partial P_R}{\partial t} \end{bmatrix}. \tag{8}$$

From the above it is evident that if $(R_0, P_{\theta_0})^\top$ are the initial conditions vector of the previous periodic solution with time T_1, then an approximation of the initial conditions vector for the next periodic solution, is $(R_0 + \delta R_0, P_{\theta_0} + \delta P_{\theta_0})^\top$. This corresponds to $T = T_1 + \varepsilon$, and it can be obtained using the solution $(\delta R_0, \delta P_{\theta_0})^\top$ of system (8). When three consecutive periodic solutions have been computed we apply Lagrange interpolation [29] to obtain a better approximation.

It is well know that the horizontal stability of a periodic orbit can be determined by the stability indices a_h, b_h, c_h and d_h [30,31]. These indices can be computed by integrating the equations of motion, for the whole period, and by making double extra integration. In particular an orbit is considered *horizontally stable* if:

$$|s_h| < 1, \quad \text{where } s_h = \begin{cases} \dfrac{a_h + d_h}{2} & \text{when the orbit is asymmetric,} \\ a_h = d_h & \text{when the orbit is symmetric.} \end{cases} \tag{9}$$

In the case where $|s_h| = 1$ the stability of the orbit is considered *critical*. For this particular case, we are able to obtain pieces of information about the family that is bifurcated. In particular when:

(i) $a_h = 1$, $b_h \neq 0$, $c_h = 0$. We have three possible cases:
- The family is not bifurcated but the characteristic curve (R_0, E) of the energy for the members of the family has an extremum.
- The family is bifurcated to simple planar symmetric families of periodic solutions.
- The family is bifurcated to simple planar symmetric families of periodic solutions and simultaneously the characteristic curve (R_0, E) of the energy for the members of the family has an extremum.

(ii) $a_h = 1$, $b_h = 0$, $c_h \neq 0$
The family is bifurcated to simple planar non-symmetric families of periodic solutions.

(iii) $a_h = -1$, $b_h \neq 0$, $c_h = 0$
The family is bifurcated to simple planar symmetric families of periodic solutions of multiplicity 2. In the representation of the basic family onto the (R_0, E) plane, the critical orbits lie on the vertical sections of the curve with the R-axis.

(iv) $a_h = -1$, $b_h = 0$, $c_h \neq 0$
The family is bifurcated to simple planar symmetric families of periodic solutions of multiplicity 2. In the representation of the basic family onto the (R_0, E) plane, the critical orbits lie on the non-vertical sections of the curve with the R-axis.

In the next section we apply the Characteristic Bisection Method to locate periodic orbits of a given multiplicity and to construct the continuation/bifurcation diagram for LiNC. The results are then compared with that of [27].

4. The characteristic polyhedron criterion and the Characteristic Bisection Method

We briefly present the *Characteristic Bisection* Method for the computation of individual members of families of periodic orbits. This method implements topological degree theory to give a criterion for the existence of an individual member of a family of periodic orbits within a given region of the phase space of the system. Then it constructs a Characteristic Polyhedron containing this member and iteratively refine this polyhedron to calculate the individual member within a predetermined accuracy. A detailed description of these procedures can be found in [19].

In general, the problem of finding periodic orbits of multiplicity p of dynamical systems in $\mathbb{R}^{n+1}$ amounts to fixing one of the variables, say $x_{n+1} = c$, for a constant c, and locating points $\mathbf{X}^* = (x_1^*, x_2^*, \ldots, x_n^*)$ on an n-dimensional surface of section Σ_{t_0} which satisfy the equation:

$$\Phi^p(\mathbf{X}^*) = \mathbf{X}^*, \tag{10}$$

where $\Phi^p = P_{t_0} : \Sigma_{t_0} \to \Sigma_{t_0}$ is the Poincaré map of the system. Obviously, this is equivalent to solving the system:

$$\mathbf{F}(\mathbf{X}) = \Phi^p(\mathbf{X}) - I_n\mathbf{X} = \mathbf{0}, \tag{11}$$

with $\mathbf{F} = (f_1, f_2, \ldots, f_n)$, where I_n is the $n \times n$ identity matrix and $\mathbf{0} = (0, 0, \ldots, 0)$ is the origin of $\mathbb{R}^n$. For example, consider a conservative dynamical system of the form:

$$\dot{\mathbf{Z}} = \mathbf{G}(\mathbf{Z}, t), \tag{12}$$

with $\mathbf{Z} = (z, \dot{z}) \in \mathbb{R}^2$ and $\mathbf{G} = (g_1, g_2)$ periodic in t with frequency ω. In this case, we can approximate periodic orbits of period p of system (12) by taking as initial conditions of these orbits the points which the orbits intersect the surface of section:

$$\Sigma_{t_0} = \left\{ \big(z(t_k), \dot{z}(t_k)\big), \text{ with } t_k = t_0 + k\frac{2\pi}{\omega},\ k \in \mathbb{N} \right\}, \tag{13}$$

at a finite number of points p. Thus, the dynamics can be studied in connection with a Poincaré map $\Phi^p = P_{t_0} : \Sigma_{t_0} \to \Sigma_{t_0}$, constructed by following the solutions of (12) in continuous time.

Suppose that $\mathbf{F}$ is continuous on the closure of a bounded domain $\mathcal{D}$ such that there is not any point $\mathbf{X}$ on its boundary for which $\mathbf{F}(\mathbf{X}) = \mathbf{0}$. Then *topological degree of* $\mathbf{F}$ *at* $\mathbf{0}$ *relative to* $\mathcal{D}$ denoted by $\deg[\mathbf{F}, \mathcal{D}, \mathbf{0}]$ and defined by

$$\deg[\mathbf{F}, \mathcal{D}, \mathbf{0}] = \sum_{\mathbf{X} \in \mathbf{F}^{-1}(\mathbf{0}) \cap \mathcal{D}} \operatorname{sgn} \det J_{\mathbf{F}}(\mathbf{X}), \tag{14}$$

where sgn is the well-known sign function with the values:

$$\operatorname{sgn} \psi = \begin{cases} -1, & \text{if } \psi < 0, \\ 0, & \text{if } \psi = 0, \\ 1, & \text{if } \psi > 0, \end{cases}$$

and $\det J_{\mathbf{F}}$ denotes the determinant of the Jacobian matrix $J_{\mathbf{F}}$ of $\mathbf{F}$. Now if $\deg[\mathbf{F}, \mathcal{D}, \mathbf{0}]$ is not equal to zero, then there is at least one solution of system (11) within $\mathcal{D}$ [16,32]. This criterion can be used, in combination with the construction of a suitable n-polyhedron, which we call Characteristic Polyhedron (CP), for the calculation of a solution contained in this region. Briefly, this can be done as follows. Let $\mathcal{M}_n$ be the $2^n \times n$ matrix whose rows are formed by all possible combinations of -1 and 1. Consider now an oriented n-polyhedron Π^n, with vertices $\mathbf{V}_k$, $k = 1, \ldots, 2^n$. If the $2^n \times n$ *matrix of signs associated with* $\mathbf{F}$ *and* Π^n, $\mathcal{S}(\mathbf{F}; \Pi^n)$, whose entries are the vectors:

$$\operatorname{sgn} \mathbf{F}(\mathbf{V}_k) = \big(\operatorname{sgn} f_1(\mathbf{V}_k), \operatorname{sgn} f_2(\mathbf{V}_k), \ldots, \operatorname{sgn} f_n(\mathbf{V}_k)\big), \tag{15}$$

is identical to $\mathcal{M}_n$, possibly after some permutations of these rows, then Π^n is called the *Characteristic Polyhedron relative to* $\mathbf{F}$. Furthermore, if $\mathbf{F}$ is continuous, then, under some suitable assumptions on the boundary of Π^n holds that:

$$\deg[\mathbf{F}, \Pi^n, \mathbf{0}] = \pm 1 \neq 0, \tag{16}$$

which implies the existence of a periodic orbit inside Π^n (see [33] for a proof). For more details on how to construct a CP and locate a desired periodic orbit see in [19,34,35]. The Characteristic Polyhedron can be considered as a translation of the Poincaré–Miranda hypercube [36–40].

Next, we describe a generalized bisection method that, in combination with the above mentioned criterion, produces a sequence of Characteristic Polyhedra of decreasing size always containing the desired solution in order to calculate it within a given accuracy (*Characteristic Bisection*). This version of bisection does not require the computation of the topological degree at each step to secure its nonzero value, as others do [41–44]. It can also be applied to problems with imprecise function values, since it depends only on their signs. The method simply amounts to constructing another refined CP, by bisecting a known one, say Π^n. We compute the midpoint $\mathbf{M}$ of a one-simplex, e.g., $\langle \mathbf{V}_i, \mathbf{V}_j \rangle$, which is one edge of Π^n. Then we obtain another CP, Π^n_*, by comparing the sign of $\mathbf{F}(\mathbf{M})$ with that of $\mathbf{F}(\mathbf{V}_i)$ and $\mathbf{F}(\mathbf{V}_j)$ and substituting $\mathbf{M}$ for that vertex for which the signs are identical [19,34, 35]. Then we continue with another edge. The number of iterations ζ required to obtain a refined Characteristic Polyhedron Π^n_* whose longest edge length, $\Delta(\Pi^n_*)$, satisfies $\Delta(\Pi^n_*) \leqslant \varepsilon$, for some accuracy $\varepsilon \in (0, 1)$, is given by [33]:

$$\zeta = \left\lceil \log_2(\Delta(\Pi^n)\varepsilon^{-1}) \right\rceil, \tag{17}$$

where the notation $\lceil \cdot \rceil$ refers to the smallest integer, which is not less than the real number quoted. Notice that ζ is independent of the dimension n and it has the same computational cost as the bisection in one-dimension which is optimal and possesses asymptotically the best rate of convergence [45].

5. Results

To produce the surface of section of the problem, we take successive sections of an orbit with the straight line $\theta = \pi$, along the positive direction of the flow ($P_\theta > 0$). In particular, we take the initial conditions (R, π, P_R, P_θ)

where the value of P_θ is computed using the equation of energy for a given value of E. Each section can be depicted as a point in the (R, P_R) plane. The transition from one section to another can be considered as a transformation in the (R, P_R) plane. Notice that, this particular transformation is well defined only if the energy E has a specific value. It is evident that a periodic orbit of period p intersects the R-axis $2p$ times. Obviously, in the simple case where $p = 1$ the orbit will be represented in the (R, P_R) plane by a single point and thereupon a p periodic orbit is represented by p points.

To compute successively the intersection points with the surface of section, we can choose a value of the energy E and by keeping this value fixed we can integrate numerically the equations of motion, using for example the Bulirsch–Stoer algorithm with proper adaptive step-size control [29,46]. These points are exhibited in Figs. 1(a)–1(f) for several initial conditions with arbitrarily chosen values of energy $E_1 = 0.005695$, $E_2 = 0.007973$, $E_3 = 0.008825$, $E_4 = 0.009112$, $E_5 = 0.011390$, $E_6 = 0.013669$ Hartree, respectively.

In Fig. 1 we can easily distinguish that there are several periodic orbits of various periods. For example, we can observe in Fig. 1(c) that the points marked by $\mathbf{P}_1$, $\mathbf{P}_2$, $\mathbf{P}_3$, $\mathbf{P}_4$ and $\mathbf{P}_5$ determine a periodic orbit of period 5.

To compute the periodic point of the period-5 orbit using the proposed Characteristic Bisection Method, we use a small box surrounding a point of the orbit, say, for example, the point $\mathbf{P}_1$ and by proper successive refinements of this box we calculate the desired point. For example, by taking the box $[4.4, 4.5] \times [0.1, 1.1]$ we have computed the included periodic point $\mathbf{P}_1 = (4.46230979, 0.67733379)^\top$. In the case of the unstable periodic point we use also a box around a region where a periodic point of the desired periodic orbit is expected to exist.

After one periodic point of the orbit has been computed, the method can be applied to obtain easily all the other periodic points of the same period to the same accuracy. More specifically, the method checks whether each mapping iteration gives a periodic point (of the same period) to the predetermined accuracy. If so, the method continues with the next iteration, otherwise it applies the process of subdivisions to a smaller box which contains the approximate periodic point. The vertices of this small box can be easily selected by permuting the components of the approximate periodic point. Using this approach we have computed all the periodic points of this orbit with coordinates:

$$\mathbf{P}_2 = (4.46230979, -0.67733379)^\top, \quad \mathbf{P}_3 = (4.51646069, -1.47786345)^\top,$$
$$\mathbf{P}_4 = (4.55104449, 0.00000000)^\top, \quad \mathbf{P}_5 = (4.51646069, 1.47786345)^\top.$$

Note that, from the sequence in which these points are created on the (R, P_R) plane, we are able to infer the rotation number of this orbit. In general, periodic orbits can be identified by their *winding* or *rotation number* σ, which is defined as follows:

$$\sigma = \frac{n_1}{n_2}, \quad n_1, n_2 \in \mathbb{N}, \tag{18}$$

where n_1, n_2, are two positive integers which indicate that the orbit has produced n_2 points, by rotating counterclockwise around the origin n_1 times [19,47]. In particular for the above periodic orbit of period 5 the value of the rotation number is:

$$\sigma = \frac{n_1}{n_2} = \frac{1}{5},$$

indicating that the orbit has produced $n_2 = 5$ points by rotating counterclockwise around the origin $n_1 = 1$ times. The values of rotation numbers for all the periodic orbits given here are exhibited in Tables 1 and 2. These values have been computed utilizing a simple angle counting procedure which we have created for this purpose.

Magnifying box A of Fig. 1(d), we observe, in Fig. 2, the existence of a periodic orbit of period 5 that is marked by $\mathbf{O}_5$. This orbit is surrounded by a group of three islands indicating the existence of another periodic orbit of period 15, marked by $\mathbf{O}_{15}$. This particular periodic orbit of period 15, required three rotations around the origin. Thus, in this case the value of the rotation number of this orbit is $\sigma = 3/15$.

We have also examined the effect of small perturbations to the initial conditions of unstable periodic orbits. For instance, by perturbing with a value $\delta_R = 10^{-5}$ the R coordinate of the unstable periodic orbit of period 3 (listed

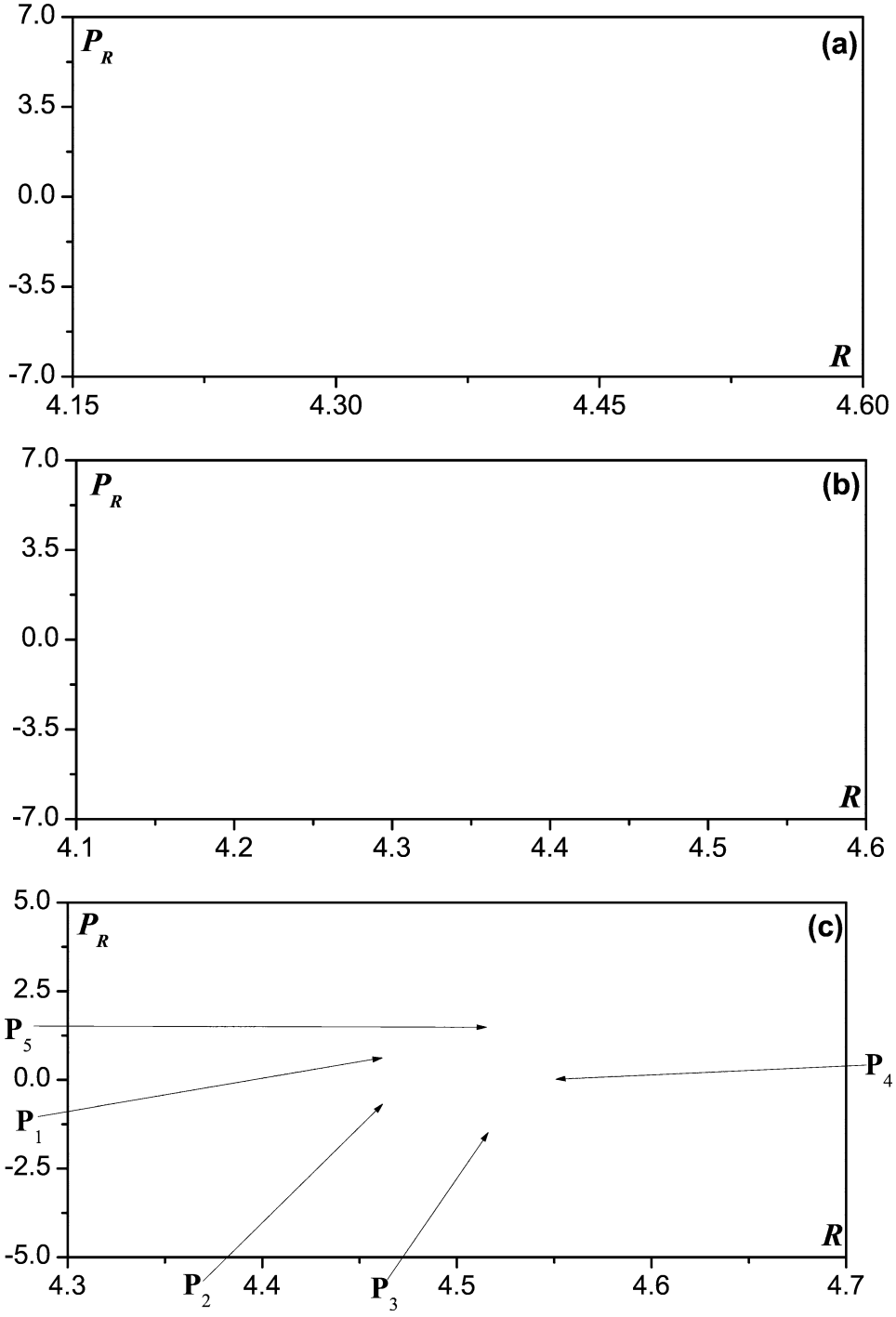

Fig. 1. Surface of section points for (a) $E_1 = 0.005695$, (b) $E_2 = 0.007973$, (c) $E_3 = 0.008825$ Hartree, respectively.

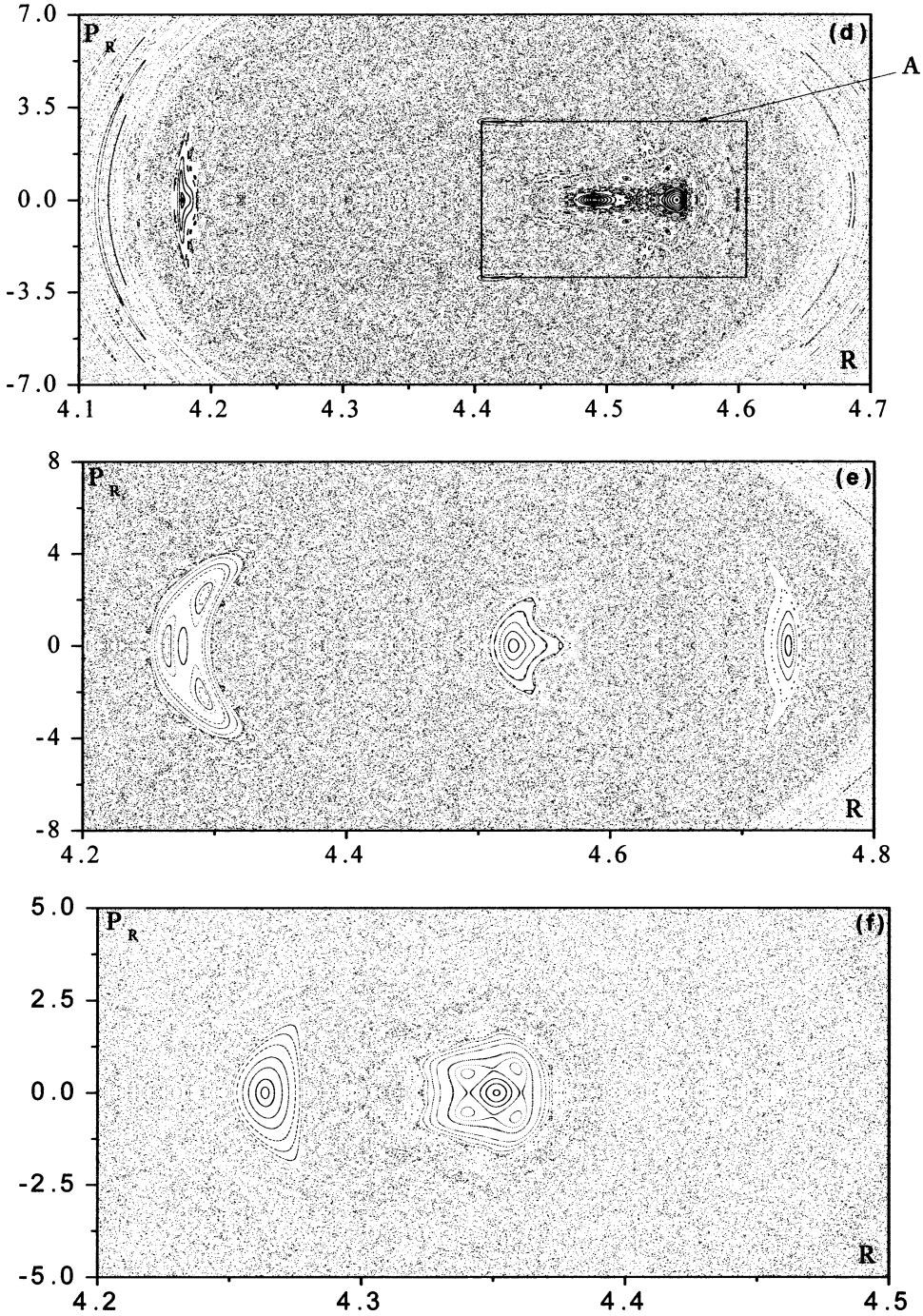

Fig. 1. (Continued). Surface of section points for (d) $E_4 = 0.009112$, (e) $E_5 = 0.011390$, and (f) $E_6 = 0.013669$ Hartree, respectively.

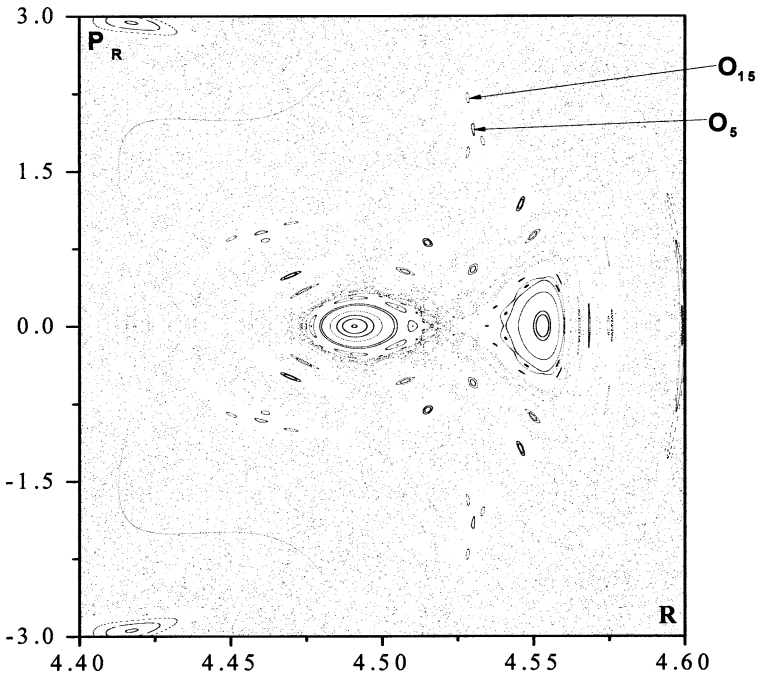

Fig. 2. Magnification of box A of Fig. 1(d). Atomic units.

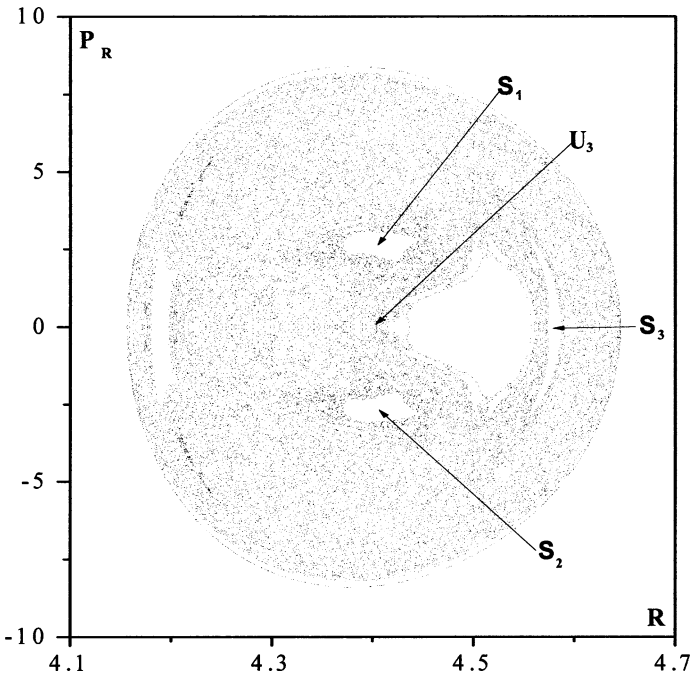

Fig. 3. Perturbations with a value $\delta_R = 10^{-5}$ of the R coordinate of the unstable period-3 periodic orbit U_3 with energy $E = 0.008825$ Hartree. S_1, S_2 and S_3 denote the corresponding period-3 stable periodic orbit.

Table 1
Fixed points of periodic orbits of period p on the Poincaré surface of section (R, P_R), within accuracy $\varepsilon = 10^{-8}$, using arbitrary values of energy E and their rotation number σ; stability index s_h and symmetry identification Sym. ("S" denotes symmetric while "A" denotes asymmetric.) Atomic units are used

E	p	Fixed point	σ	s_h	Sym
0.005695	1	(4.28484649, 0.00000000)	1	0.57372	S
0.005695	1	(4.38896972, 0.00000000)	1	−0.00711	S
0.005695	1	(4.19475004, 0.00000000)	1	0.67680	S
0.007973	1	(4.46165957, 0.00000000)	1	0.02763	S
0.007973	1	(4.22049227, 0.00000000)	1	−0.68166	S
0.008825	1	(4.51069744, 0.00000000)	1	0.82954	S
0.009112	1	(4.17833963, 0.00000000)	1	−0.56050	S
0.009112	1	(4.49082546, 0.00000000)	1	0.33794	S
0.009112	1	(4.55303293, 0.00000000)	1	0.33793	S
0.011390	1	(4.22563562, 0.00000000)	1	−0.34420	S
0.011390	1	(4.47645058, 0.00000000)	1	−0.24644	S
0.011390	1	(4.68497334, 0.00000000)	1	−0.24644	S
0.013669	1	(4.26348970, 0.00000000)	1	0.03415	S
0.013669	1	(4.35124581, 0.00000000)	1	−0.99770	S
0.013669	2	(4.34008538, 0.52849407)	1/2	0.96772	A
0.013669	2	(4.34988026, 0.63067602)	1/2	1.01725	A
0.007973	3	(4.34316520, 3.97679118)	2/3	0.98244	A
0.008825	3	(4.58187805, 0.00000000)	1/3	−0.85018	S
0.008825	3	(4.40329072, 0.00000000)	1/3	6.66521	S
0.009112	3	(4.59912193, 0.00000000)	1/3	0.04945	S
0.011390	3	(4.21309824, 0.00000000)	2/3	0.68157	S
0.011390	3	(4.23422106, 0.00000000)	2/3	1.20225	S

in Tables 1 and 2 with energy $E = 0.008825$) and marked by $\mathbf{U}_3$ in Fig. 3 we observe that the iterations of the perturbed orbit diffuse away from the point $\mathbf{U}_3$ surrounding also the stable orbit of period 3.

In Tables 1 and 2 we exhibit several fixed points of periodic orbits of period p on the Poincaré surface of section for the LiNC model using several values of the energy, with an accuracy of $\varepsilon = 10^{-8}$. Also, in this table we give the corresponding rotation numbers σ. In addition, in this table we give the stability index s_h as they are defined in Eq. (9) as well as the symmetry identification of the corresponding orbit.

We have calculated the continuation/bifurcation diagram of LiNC up to energies of 5000 cm^{-1} by using the CBM. In Fig. 4 we show the projection of the continuation/bifurcation diagram in the (E, R) plane which can be compared with that of Fig. 1 of the [27]. In the new diagram we also show eight new families of periodic orbits located with the CBM. In Table 3 we give initial conditions for one periodic orbit of each new family and in Fig. 5 we show their morphologies. In the continuation scheme we kept the angle coordinate θ equal to π. The stable principal family which corresponds to the stretch mode of the system is not shown but only the **B** principal

Table 2
(Continuation of Table 1)

E	p	Fixed point	σ	s_h	Sym
0.008825	5	(4.55104449, 0.00000000)	1/5	−0.24616	S
0.008825	5	(4.45167525, 0.00000000)	1/5	2.74075	S
0.009112	5	(4.57595772, 0.00000000)	1/5	−0.41051	S
0.009112	5	(4.44349025, 0.00000000)	1/5	12.09241	S
0.009112	6	(4.54083980, 0.12064771)	1/6	0.79060	A
0.009112	6	(4.54019427, 0.00000000)	1/6	1.19786	S
0.009112	6	(4.51009863, 0.00000000)	1/6	0.79059	S
0.009112	6	(4.50856645, −0.09298509)	1/6	1.19787	A
0.007973	7	(4.34009828, 4.40878879)	5/7	0.26382	A
0.007973	7	(4.38098920, 4.34966352)	5/7	1.04861	A
0.008825	7	(4.59574144, 0.00000000)	3/7	−0.66944	S
0.009112	7	(4.56843550, 0.00000000)	1/7	−0.83431	S
0.009112	7	(4.45804429, 0.00000000)	1/7	10.09958	S
0.011390	7	(4.19802601, 0.00000000)	4/7	−0.87763	S
0.011390	7	(4.24856583, 0.00000000)	4/7	11.90610	S
0.009112	8	(4.18234538, −1.19641052)	3/8	0.72551	A
0.009112	8	(4.17264206, 0.00000000)	3/8	0.72570	S
0.009112	9	(4.56516170, 0.00000000)	1/9	−0.88784	S
0.009112	9	(4.46528109, 0.00000000)	1/9	9.59461	S
0.011390	10	(4.51232428, 0.00000000)	7/10	0.85615	S
0.011390	10	(4.49147743, 1.84209780)	7/10	1.12108	A
0.007973	11	(4.52112213, 0.00000000)	3/11	0.56407	S
0.007973	11	(4.34305487, 0.00000000)	3/11	1.45503	S
0.009112	13	(4.18891990, 0.00000000)	5/13	−0.88146	S
0.009112	13	(4.17193325, 0.00000000)	5/13	5.19234	S
0.009112	15	(4.57472227, 0.00000000)	3/15	−0.02211	S
0.009112	15	(4.57628775, 0.00000000)	3/15	1.12375	S
0.008825	28	(4.52039403, −2.55562870)	7/28	0.83668	A
0.008825	28	(4.52306399, −2.33238052)	7/28	1.15107	A

family which describes the bend mode of the molecule. Bifurcating families are labeled with numbers and the two branches with the letters **A** and **B**. In Figs. 6(a)–6(b) we exhibit asymmetric families of periodic orbits which individual members have been computed by CBM. The morphologies of the corresponding individual members are depicted in Figs. 6(c)–6(d).

The stability properties of the **B** family and its bifurcations found with the Newton method are reproduced. Particularly, the early transition to instability at 733.2 cm^{-1}, after which it turns stable again. Other instability

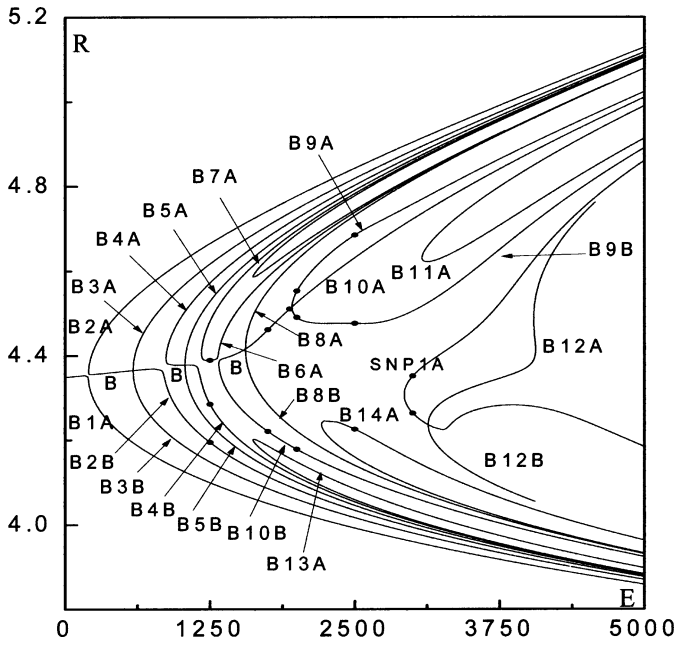

Fig. 4. The continuation/bifurcation diagram of LiNC up to energies of 5000 cm^{-1} obtained by the CBM. The dots indicate the corresponding individual members (listed in Table 1) of the families.

Table 3
Periodic orbits of the new families of Fig. 4. Energy in cm^{-1} and all other quantities in atomic units

	E	$T/2$	R	P_θ	a_h	b_h	c_h
B12A-B12B	3998.71145	8564.22317	4.37452189	39.78983800	103.98479	−20.05839	−539.01854
B3A-B3B	3529.30741	6733.27742	4.94950000	11.17590706	0.96912	−0.00001	7231.94073
B5A-B5B	2205.35916	8609.36622	4.74350000	15.78909127	0.74578	−0.00011	3878.54789
B8A-B8B	2200.77283	9195.65039	4.18450000	26.40552493	9.23215	−0.03423	−2460.96287
B7A	1930.73612	10846.32026	4.67230000	18.12009369	0.06735	−0.00050	1985.77618
B13A	1673.86664	10930.62244	4.18280000	22.11094069	0.86852	−0.00013	1898.19939
B14A	2445.61396	7795.76681	4.23250000	29.64408555	−0.61478	0.00433	−143.71027
B11A	4263.01575	8135.65105	4.79600000	30.68000219	10.41481	−0.03763	−2855.87964

regions were located at 1034.6 and 1543.8 cm^{-1}, but it permanently becomes unstable at the energy of 1958.6 cm^{-1}.

The interesting bifurcations of the **B** family at 201.7, 870.7, 1176.4, and 1326.5 cm^{-1}, which give rise to the families B1, B2, B4, B7 and B10, respectively are reproduced. As it is shown in Fig. 4, the principal **B** family at these bifurcation points shows characteristic *gaps* in its continuation diagram. A gap appears since the principal family is smoothly split and it is connected with the two bifurcating families, branches **A** and **B**. Contopoulos [48] has studied this phenomenon on a 2D rotating galactic model type potential. He showed that gaps in the continuation diagram appear in the cases of $n/1$ (n even) resonance conditions between the two characteristic frequencies of the Hamiltonian. In our case, we can see from the morphologies of the bifurcating

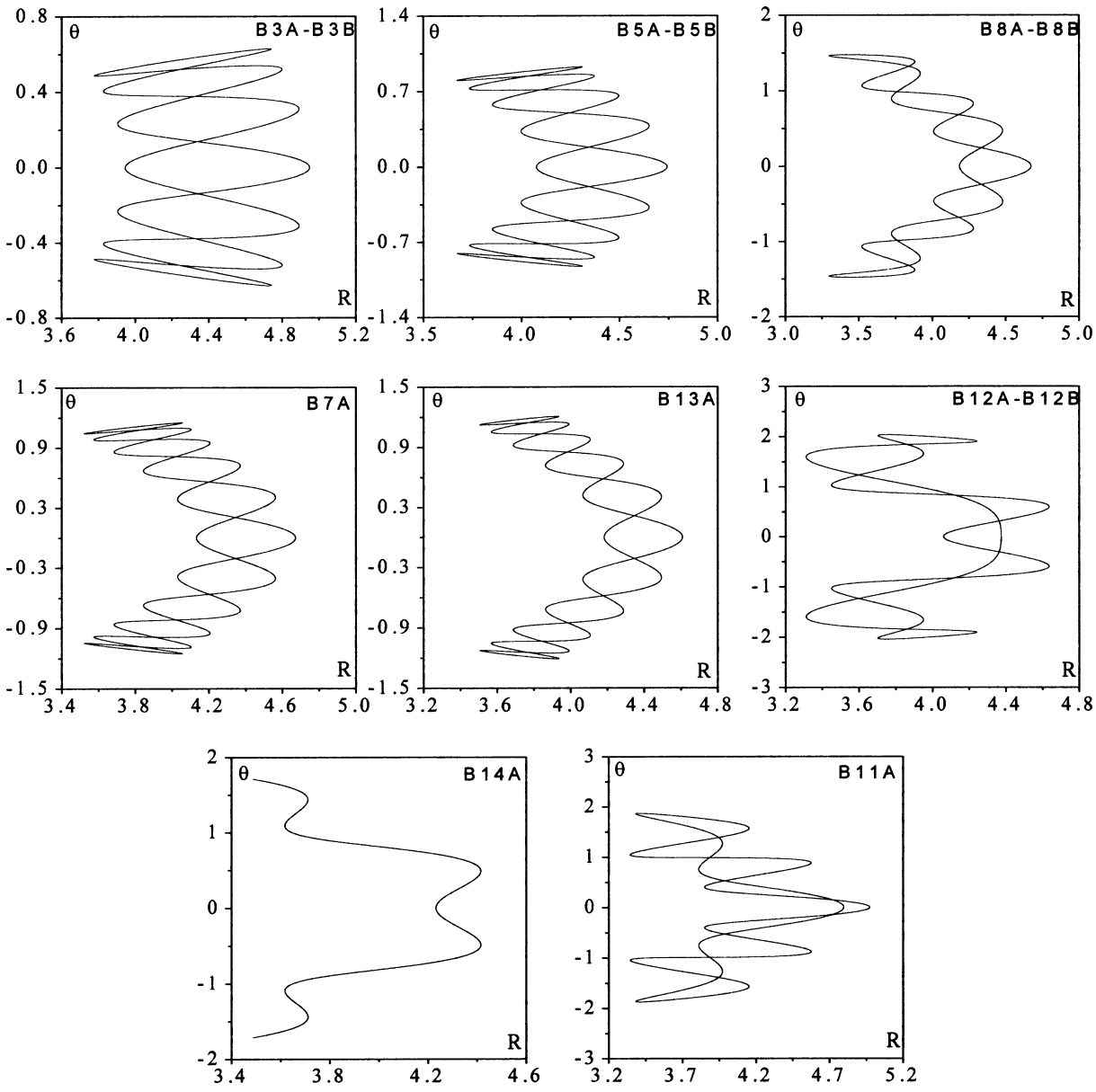

Fig. 5. Representative periodic orbits of the New families in the (R, θ) plane.

periodic orbits that the resonances which are responsible for the gaps are the 6/1 (**B1A**, **B1B**), 8/1 (**B2A**, **B2B**), and 10/1 (**B4A**, **B4B**).

A systematic study of the morphologies of the **B** type periodic orbits reveals that their shapes change significantly at energies above the last gap. It is worth mentioning that this energy is above the plateau (about 1207 cm^{-1}). Also, all the bifurcating periodic orbits from the **B** principal family appear with the same period as the parent one, and that means, that one pair of eigenvalues of the monodromy matrix is equal to one. The only exception is the **B8A**

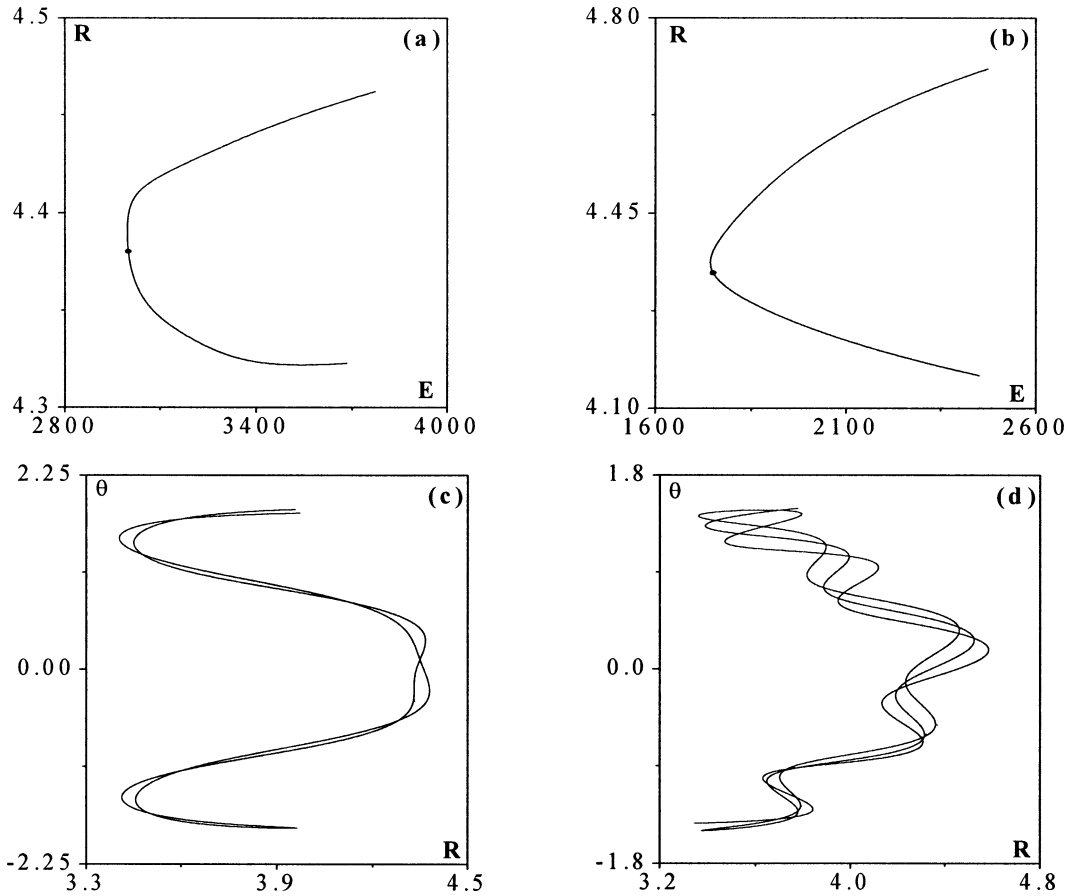

Fig. 6. Families of asymmetric periodic orbits and the morphologies of their individual members. (a) Family of asymmetric periodic orbits with initial condition $(x, \dot{x}) = (4.34008538, 0.52849407)$ with energy $E = 0.013669$ (Table 1), (b) family of asymmetric periodic orbits with initial condition $(x, \dot{x}) = (4.34316520, 3.97679118)$ with energy $E = 0.007973$ (Table 1), (c) the morphology of an individual member of the family in Fig. 6(a) and (d) the morphology of an individual member of the family in Fig. 6(b).

family (Fig. 4) that has a double period (one pair of eigenvalues of the monodromy matrix of the parent family is equal to -1). The new families are mainly periodic orbits of high multiplicity as it is shown in Fig. 5.

6. Conclusions

The floppy molecule LiNC/LiCN has an interesting and complicate bifurcation diagram with gaps for the principal family associated with the bend vibrational mode of the system. Hence, we have employed this system to test a new method for finding periodic orbits and producing the bifurcation diagram. The Characteristic Bisection Method exploits topological degree theory to provide a criterion for the existence of a periodic orbit of an iterate of the mapping within a given region. The method constructs a polyhedron in such a way that the value of the topological degree of an iterate of the mapping relative to this polyhedron is ± 1, which means that there exists a periodic orbit within this polyhedron. Then, by using a generalized bisection method we subdivide an edge or a diagonal of the polyhedron to restrict the periodic orbit in a smaller region and iteratively to converge to the desired accuracy.

Apart from reproducing previous results obtained by the Multiple Shooting algorithm, we have also found new families of periodic orbits of high multiplicity. The CBM seems to be robust enough to be applied to larger molecular systems results on which will be presented in a future publication.

References

[1] S.C. Farantos, Int. Rev. Phys. Chem. 15 (1996) 345.
[2] H.S. Taylor, in: H.-L. Dai, R.W. Field (Eds.), Molecular Dynamics and Spectroscopy by Stimulated Emission Pumping, World Scientific, Singapore, 1995, p. 891.
[3] J.M. Gomez Llorente, E. Pollak, Ann. Rev. Phys. Chem. 43 (1992) 91.
[4] M. Founargiotakis, S.C. Farantos, G. Contopoulos, C. Polymilis, J. Chem. Phys. 91 (1989) 1389.
[5] S.C. Farantos, M. Founargiotakis, C. Polymilis, Chem. Phys. 135 (1989) 347.
[6] H. Ishikawa, R.W. Field, S.C. Farantos, M. Joyeux, J. Koput, C. Beck, R. Schinke, HCP–CPH Isomerization: Caught in the Act, Ann. Rev. Phys. Chem. 50 (1999) 443.
[7] M.P. Jacobson, H.S. Taylor, C. Jung, R.W. Field, J. Chem. Phys. 109 (1998) 121.
[8] R. Prosmiti, S.C. Farantos, J. Chem. Phys. 103 (1995) 3299.
[9] M.C. Cutzwiller, Chaos in Classical and Quantum Mechanics, Springer, New York, 1990.
[10] M.E. Kellman, Ann. Rev. Phys. Chem. 48 (1995) 398.
[11] S.C. Farantos, H.-M. Keller, R. Schinke, K. Yamashita, K. Morokuma, J. Chem. Phys. 104 (1996) 10 055.
[12] Ch. Beck, H.-M. Keller, S.Yu. Grebenshchikov, R. Schinke, S.C. Farantos, K. Yamashita, K. Morokuma, J. Chem. Phys. 107 (1997) 9818.
[13] R. Seydel, From Equilibrium to Chaos: Practical Bifurcation and Stability Analysis, Elsevier, Amsterdam, 1988.
[14] S.C. Farantos, Comput. Phys. Comm. 108 (1998) 240.
[15] V.V. Markellos, W. Black, P.E. Moran, Celest. Mech. 9 (1974) 507.
[16] J.M. Ortega, W.C. Rheinbolt, Iterative solution of nonlinear equations in several (1970).
[17] J.E. Dennis, R.B. Schnabel, Numerical Methods for Unconstrained Optimization and Nonlinear Equations, SIAM, Philadelphia, 1996.
[18] G.S. Androulakis, M.N. Vrahatis, J. Comput. Appl. Math. 72 (1996) 41.
[19] M.N. Vrahatis, J. Comput. Phys. 119 (1995) 105.
[20] L. Drossos, O. Ragos, M.N. Vrahatis, T.C. Bountis, Phys. Rev. E 53 (1996) 1206.
[21] M.N. Vrahatis, T.C. Bountis, M. Kollmann, Inter. J. Bifurc. Chaos 6 (1996) 1425.
[22] M.N. Vrahatis, H. Isliker, T.C. Bountis, Inter. J. Bifurc. Chaos 7 (1997) 2707.
[23] H. Waalkens, J. Wiersig, H.R. Dullin, Ann. Phys. 260 (1997) 50.
[24] N. Burić, M. Mudrinić, J. Phys. A: Math. Gen. 31 (1998) 1875.
[25] N. Burić, M. Mudrinić, Todorović, J. Phys. A: Math. Gen. 31 (1998) 7847.
[26] V.S. Kalantonis, E.A. Perdios, A.E. Perdiou, M.N. Vrahatis, Celest. Mech. Dynam. Astron. (2001), in press.
[27] R. Prosmiti, S.C. Farantos, R. Guantes, F. Borondo, R.M. Benito, J. Chem. Phys. 104 (1996) 2921.
[28] R. Essers, J. Tennyson, P.E.S. Wormer, Chem. Phys. Lett. 89 (1982) 223.
[29] W.H. Press, S.A. Teukolsky, W.T. Vetterling, B.P. Flannery, Numerical Recipes, The Art of Scientific Computing, 2nd edn., Cambridge University Press, New York, 1992.
[30] M. Hénon, Astron & Astrophys. 28 (1973) 415.
[31] V.V. Markellos, Astrophys. Space Sci. 43 (1976) 449.
[32] N.G. Lloyd, Degree Theory, Cambridge University Press, Cambridge, 1978.
[33] M.N. Vrahatis, K.I. Iordanidis, Numer. Math. 49 (1986) 123.
[34] M.N. Vrahatis, ACM Trans. Math. Software 14 (1988) 312.
[35] M.N. Vrahatis, ACM Trans. Math. Software 14 (1988) 330.
[36] H. Poincaré, C. R. Acad. Sci. Paris 97 (1883) 251.
[37] H. Poincaré, Bull. Astronomique 1 (1884) 63.
[38] C. Miranda, Bol. Un. Mat. Ital. 3 (1940) 5.
[39] M.N. Vrahatis, Proc. Amer. Math. Soc. 107 (1989) 701.
[40] W. Kulpa, Amer. Math. Monthly 104 (1997) 545.
[41] R.B. Kearfott, Numer. Math. 32 (1979) 109.
[42] A. Eiger, K. Sikorski, F. Stenger, ACM Trans. Math. Software 10 (1984) 367.
[43] M.N. Vrahatis, Bull. Soc. Math. Grèce 27 (1986) 161.
[44] J.M. Greene, J. Comput. Phys. 98 (1992) 194.
[45] K. Sikorski, Numer. Math. 40 (1982) 111.
[46] J. Stoer, R. Bulirsch, Introduction to Numerical Analysis, Springer, New York, 1980.
[47] J.M. Greene, J. Math. Phys. 20 (1979) 1183.
[48] G. Contopoulos, Physica D 8 (1983) 142.